

Effects of coupling between octahedral tilting and polar modes on the phase diagram of $\text{PbZr}_{1-x}\text{Ti}_x\text{O}_3$

F. Cordero,¹ F. Trequattrini,² F. Craciun¹ and C. Galassi³

¹ CNR-ISC, Istituto dei Sistemi Complessi, Area della Ricerca di Roma - Tor Vergata, Via del Fosso del Cavaliere 100, I-00133 Roma, Italy

² Dipartimento di Fisica, Università di Roma "La Sapienza", P.le A. Moro 2, I-00185 Roma, Italy and

³ CNR-ISTEC, Istituto di Scienza e Tecnologia dei Materiali Ceramici, Via Granarolo 64, I-48018 Faenza, Italy

(Dated:)

The results are presented of anelastic and dielectric spectroscopy measurements on large grain ceramic $\text{PbZr}_{1-x}\text{Ti}_x\text{O}_3$ (PZT) with compositions near the two morphotropic phase boundaries (MPBs) that the ferroelectric (FE) rhombohedral phase has with the Zr-rich antiferroelectric and Ti-rich FE tetragonal phases. These results are discussed together with similar data from previous series of samples, and reveal new features of the phase diagram of PZT, mainly connected with octahedral tilting and its coupling with the polar modes. Additional evidence is provided of what we interpret as the onset of the tilt instability, when is initially frustrated by lattice disorder, and the long range order is achieved at lower temperature. Its temperature $T_{\text{IT}}(x)$ prosecutes the long range tilt instability line $T_{\text{T}}(x)$ up to T_{C} , when T_{T} drops. It is proposed that the difficulty of seeing the expected $\frac{1}{2}\langle 111 \rangle$ modulations in diffraction experiments is due to the large correlation volume associated with that type of tilt fluctuations combined with strong lattice disorder.

It is shown that the lines of the tilt instabilities tend to be attracted and merge with those of polar instabilities. Not only T_{IT} bends toward T_{C} and then merges with it, but in our series of samples the temperature T_{MPB} of the dielectric and anelastic maxima at the rhombohedral/tetragonal MPB does not cross T_{T} , but deviates remaining parallel or possibly merging with T_{T} . These features, together with a similar one in $(\text{Na}_{1/2}\text{Bi}_{1/2})_{1-x}\text{Ba}_x\text{TiO}_3$, are discussed in terms of cooperative coupling between tilt and FE instabilities, which may trigger a common phase transition. An analogy is found with recent simulations of the tilt and FE transitions in multiferroic BiFeO_3 [Kornev and Bellaiche, Phys. Rev. B **79**, 100105 (2009)].

An abrupt change is found in the shape of the anelastic anomaly at T_{T} when x passes from 0.465 to 0.48, possibly indicative of a rhombohedral/monoclinic boundary.

I. INTRODUCTION

The phase diagram of the most widely used ferroelectric perovskite $\text{PbZr}_{1-x}\text{Ti}_x\text{O}_3$ (PZT) still has unclear features (for the phase diagram, see Fig. 7). It has been known since the fifties¹⁻³ and the major recent discovery was the existence of a monoclinic (M) phase⁴ in a narrow region at the morphotropic phase boundary (MPB) that separates the ferroelectric (FE) Zr-rich rhombohedral (R) region from the Ti-rich tetragonal (T) one. In the M phase the polarization may in principle continuously rotate between the directions in the T and R domains, so providing an additional justification for the well known and exploited maximum of the electromechanical coupling at the MPB. The existence of domains of M phase is actually still debated, the alternative being nanotwinned R and/or T domains that over a mesoscopic scale appear as M.^{5,6} Since experimental evidences for both types of structures exist, the possibility should be considered that genuine M domains and nanotwinning coexist at the MPB, being both manifestations of a free energy that becomes almost isotropic with respect to the polarization.⁷ The part of the MPB line below room temperature has been investigated only after the discovery of the M phase, and is reported to go almost straight to 0 K at $x \simeq 0.52$.^{8,9}

Recent studies are also revealing new features of how

the TiO_6 and ZrO_6 octahedra tilt at low temperature. The instability of the octahedral network toward tilting is a common phenomenon in perovskites ABO_3 , usually well accounted for by the mismatch between the network of B-O bonds with that of A-O bonds which are softer and with larger thermal expansion.^{14,15} In these cases, lowering temperature or increasing the average B size sets the stiff B-O network in compression, which is relieved by octahedral tilting.¹⁰⁻¹³ In the case of PZT, Zr has a radius 19% smaller than Ti and one expects the tilt instability to occur below a $T_{\text{T}}(x)$ line that encloses the low- T and low- x corner of the $x - T$ phase diagram. Indeed, the Zr-rich antiferroelectric compositions are tilted ($a^-a^-c^0$ in Glazer's notation,¹⁶ meaning rotations of the same angle about two pseudocubic axes in anti-phase along each of them and no rotation around the third axis), below a $T_{\text{AF}}(x)$ line that goes steeply toward 0 K at $x \sim 0.05$. Also at higher Ti compositions tilting is observed ($a^-a^-a^-$ compatible with the rhombohedral $R3c$ structure) below a T_{T} line that presents a maximum at $x \sim 0.16$ and whose prosecution to low temperature was not followed beyond $x = 0.4$ until recently. The prediction from first principles calculations that octahedral tilting occurs also in the M and T phase¹⁷ has been confirmed by anelastic and dielectric,¹⁸ structural,¹⁹ Raman²⁰ and infra-red²¹ experiments. The presence of a low-temperature monoclinic Cc phase²² with tilt pattern $a^-a^-c^-$ intermediate between tilted R and T has been

excluded by a recent neutron diffraction experiment on single crystals,²³ where below T_T coexistence was found of tilted $R3c$ and untilted Cm phases. Yet, evidence for the Cc phase has been subsequently reported on PZT where 6% Pb was substituted with smaller Sr, in order to enhance tilting.²⁴

Here we report the results of anelastic and dielectric experiments at additional compositions with respect to our previous investigations, which reveal new features of the phase diagram of PZT, mainly related to octahedral tilting and its coupling with the polar degrees of freedom.

II. EXPERIMENTAL

Large grain (average sizes 15–30 μm) ceramic samples of $\text{PbZr}_{1-x}\text{Ti}_x\text{O}_3$, with nominal compositions $x = 0.05, 0.062, 0.08, 0.12, 0.40, 0.487, 0.494$ have been prepared with the mixed-oxide method in the same manner as previous series of samples.^{7,18} The starting oxide powders were calcined at 800 °C for 4 hours, pressed into bars and sintered at 1250 °C for 2 h, packed with $\text{PbZrO}_3 + 5\text{wt}\%$ excess ZrO_2 to prevent PbO loss during sintering. The powder X-ray diffraction did not reveal any trace of impurity phases and the densities were about 95% of the theoretical ones. The sintered blocks were cut into thin bars 4 cm long and 0.6 mm thick for the anelastic and dielectric experiments and discs with a diameter of 13 mm and a thickness of 0.7 mm were also sintered only for the dielectric measurements. The faces were made conducting with Ag paste.

The dielectric susceptibility $\chi(\omega, T) = \chi' - i\chi''$ was measured with a HP 4194 A impedance bridge with a four wire probe and an excitation of 0.5 V/mm, between 0.1 and 100 kHz. The heating and cooling runs were made at 0.5–1.5 K/min between 100 and 800 K in a modified Linkam HFS600E-PB4 stage and up to 540 K in a Delta climatic chamber.

The dynamic Young's modulus $E(\omega, T) = E' + iE''$ was measured between 100 and 770 K in vacuum by electrostatically exciting the flexural modes of the bars suspended on thin thermocouple wires.²⁵ The reciprocal of the Young's modulus, the compliance $s = s' - is'' = 1/E$, is the mechanical analogue of the dielectric susceptibility. During a same run the first three odd flexural vibrations could be excited, whose frequencies are in the ratios 1 : 5.4 : 13.2. The angular frequency of the fundamental resonance is²⁶ $\omega \propto \sqrt{E'}$, and the temperature variation of the real part of the compliance is given by $s(T)/s_0 \simeq \omega_0^2/\omega^2(T)$, where ω_0 is chosen so that s_0 represents the compliance in the paraelectric phase. The imaginary parts of the susceptibilities contribute to the losses, which are presented as $Q^{-1} = s''/s'$ for the mechanical case and $\tan \delta = \chi''/\chi'$ for the dielectric one.

III. RESULTS

For clarity, we will consider separately the anelastic and dielectric spectra with compositions in the range $0.05 < x < 0.2$, and those in the MPB region. We will present the new data together with those already published in Ref. 18 ($x = 0.455, 0.465, 0.48, \text{ and } 0.53$) and Ref. 7 ($x = 0.1, 0.14, 0.17, 0.42, 0.45, 0.452$).

A. Octahedral tilting below T_T and T_{TT} : $0.062 < x < 0.2$

Figure 1 presents the dielectric and anelastic spectra measured during heating of $\text{PbZr}_{0.92}\text{Ti}_{0.08}\text{O}_3$, a composition where also the new transition at T_{TT} is clearly visible in the elastic compliance s' . The comparison between the two types of susceptibilities puts in evidence their complementarity in studying combinations of polar and non polar modes. The dielectric susceptibility χ' is of course dominated by the FE transition at T_C (note the logarithmic scale), it has a very attenuated step below the well known tilt transition at T_T , and practically nothing visible at T_{TT} , due to both the broader shape of the anomaly and the proximity to the Curie-Weiss peak. The dielectric losses provide an indirect but more clear mark of the non polar transition at T_T , presumably through a change in the mobility and/or amplitude of charge and polar relaxations which are affected by octahedral tilting.

The effect of cooling through T_T on the dielectric susceptibility is more convincingly shown to be a positive step in Fig. 2, and this fact will be discussed as a sign of cooperative coupling between tilt and polar modes.

The elastic compliance s' , on the other hand, is only indirectly affected by the FE transition, since strain is not an order parameter of the transition and is linearly coupled to the square of the polarization. The Landau theory of phase transitions^{27,28} predicts a step in s' for this type of coupling, which is indeed observed at higher Ti compositions,¹⁸ but has a strong peaked component in Zr-rich PZT. We do not have an obvious explanation for this peaked response, which is frequency independent and intrinsic, but mechanisms involving dynamical fluctuations of the order parameter coupled with strain are possible.²⁸ The advantage of a reduced anelastic response to the FE instabilities is that the other transitions are not as masked as in the dielectric case, so that not only is the tilt transition at T_T clearly visible as a step in s' and peak in Q^{-1} , but also the new transition can be detected at T_{TT} even very close to T_C . As already discussed,⁷ this transition has all the features of the transition at T_T but the associated anomaly is attenuated and broadened, so providing further support to an explanation in terms of a disordered precursor to the final long range tilt ordering below T_T .

The broad peaks and steps in both the dielectric and anelastic losses below T_C have scarce reproducibility, which indicates their extrinsic origin, namely the motion

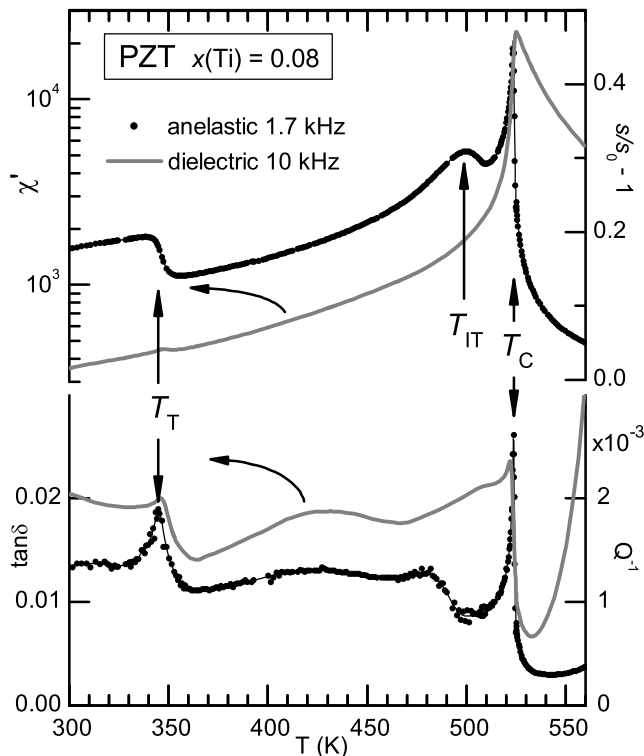


FIG. 1: Dielectric (left ordinates) and anelastic (right ordinates) spectra (higher panel real susceptibilities, lower panel losses) of $\text{PbZr}_{0.92}\text{Ti}_{0.08}\text{O}_3$ measured during heating.

of domain walls and charged defects, whose state depends on the thermal history. Instead, all the features indicated by arrows are completely independent of the measuring frequency, temperature rate and thermal history, and therefore are recognizable as intrinsic effects due to the FE and tilt transitions. Hysteresis between heating and cooling is observed due to the first order character of the transitions and to the presence of domain walls relaxations. Examples of the differences between the features that are intrinsic and stable and those that present dispersion in frequency or are less reproducible have been reported previously^{7,18} and are omitted here.

Figure 3 presents the anelastic spectra of PZT with $0.062 < x < 0.17$, including compositions already present in Ref. 7. All the curves are similar to the $x = 0.08$ case of Fig. 1, with the three type of transitions at T_C , T_{IT} and T_T clearly visible in separate temperature ranges. Both the s' and Q^{-1} curves have sharp peaks at the FE transitions, so that the T_C 's are simply labeled with the compositions in %Ti. The other transition temperatures are indicated by vertical bars centered on the curves and arrows labeled with the respective compositions. The features of Q^{-1} in the T_{IT} temperature range are not labeled because are due to the extrinsic contributions mentioned above.

The temperatures of the tilt transition are identified with the upper edges of the steps in the real parts, which generally coincide with a spike or sharp kink in the losses.

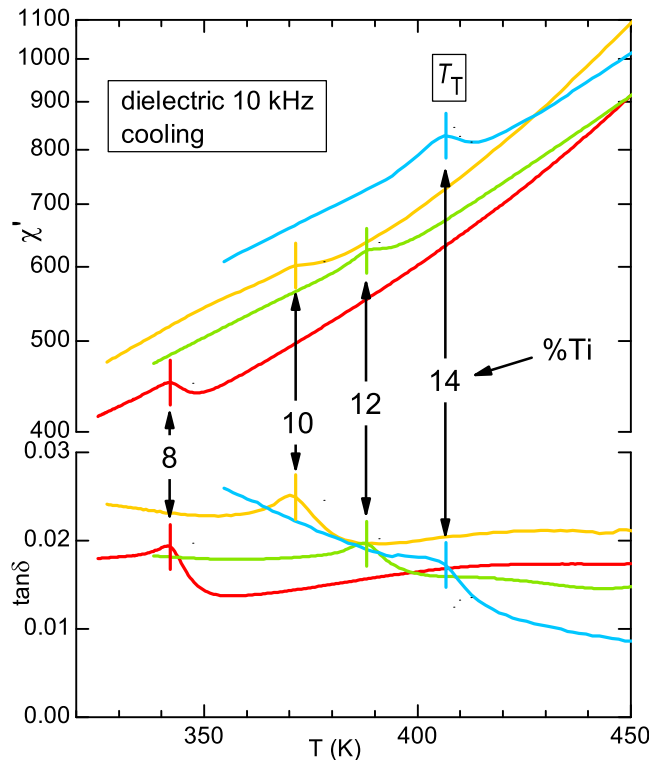


FIG. 2: (Color online) Dielectric susceptibility and loss of $\text{PbZr}_{1-x}\text{Ti}_x\text{O}_3$ measured during cooling through the tilt transition.

The rounded step and lack of reproducible anomaly in the losses increase the error on T_{IT} , which however remains small enough to not change the features of the phase diagram discussed later. Due to the importance of the behavior of $T_{IT}(x)$ in the Discussion, a detail of this anomaly in the $s'(T)$ curves, including 5% Ti, is shown in Fig 4. An anomaly corresponding to T_{IT} might be present slightly above T_T for $x = 0.17$, but lacking a clear sign of it, it is assumed to coincide with T_T . At low x , the curve of $x = 0.05$ does not present any clear shoulder below T_C , and it is assumed $T_{IT} \equiv T_C$.

The transition temperatures measured on both heating and cooling are reported in the phase diagram of Fig. 7, where the T_{IT} line departs from T_T at $x \simeq 0.17$, has a kink centered at $x = 0.11$ and finally joins the T_C line at $0.05 < x < 0.062$. The new feature that will be the main focus of the present work is the kink and the merging with T_C at $x > 0.05$. It is also noticeable that the anomaly at T_{IT} becomes more intense and sharper on approaching T_C .

B. Compositions near the MPB

As discussed in the previous investigations,^{7,18} the MPB in PZT is signaled by a maximum in the dielectric and above all elastic susceptibilities. Again, it is stressed that such maxima are almost independent of fre-

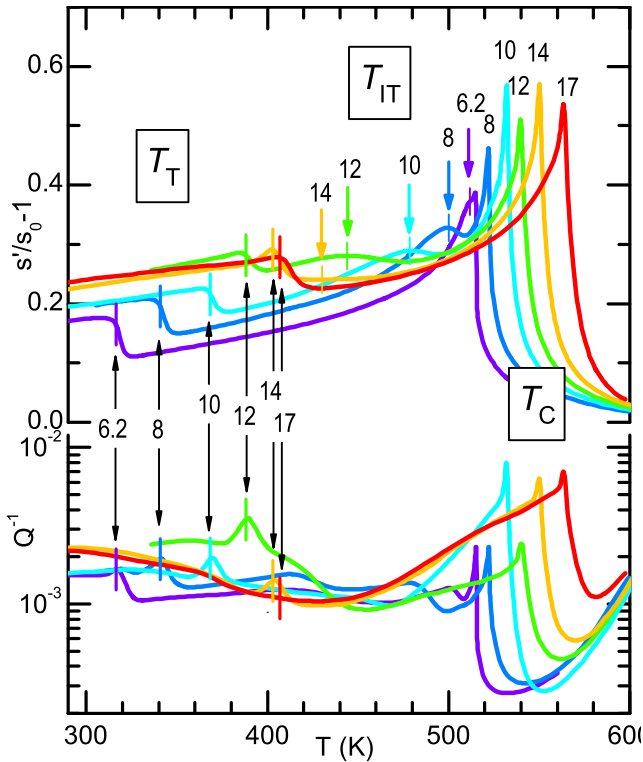


FIG. 3: (Color online) Elastic compliance s' and energy loss coefficient Q^{-1} measured at ~ 1.7 kHz on PZT at the compositions 6.2, 8, 10, 12, 14, 17% Ti, as indicated by the numbers at the phase transitions. The curves of 10, 14 and 17% Ti are from Ref. 7.

quency and temperature rate, and therefore are intrinsic effects due to the evolution of the order parameter at the MPB and its coupling with strain. Also the losses are rather high in the region of the MPB, but no feature is found that is directly ascribable to the phase transition; rather, their dependence on frequency and thermal history show that they are due to the abundant twin walls and other domain boundaries, whose density and mobility depend on many factors and is maximal around the MPB. Instead, the losses contain clear cusps or steps at the tilt transitions,^{7,18} so allowing T_T to be determined also in the proximity with the MPB, where the real part is dominated by the peak at T_{MPB} . We therefore discuss separately the real parts of χ and s , containing information on the polar transition at the MPB, and the losses, containing information on the tilt transitions.

C. Maxima of the susceptibilities at the MPB

Figure 5 is an overview of χ' and s' curves measured during cooling at all the compositions $x \geq 0.40$ we tested so far.

We call T_{MPB} the temperatures of the maxima in χ' and s' , marked with vertical bars on the curves. These temperatures do not coincide exactly with each other,

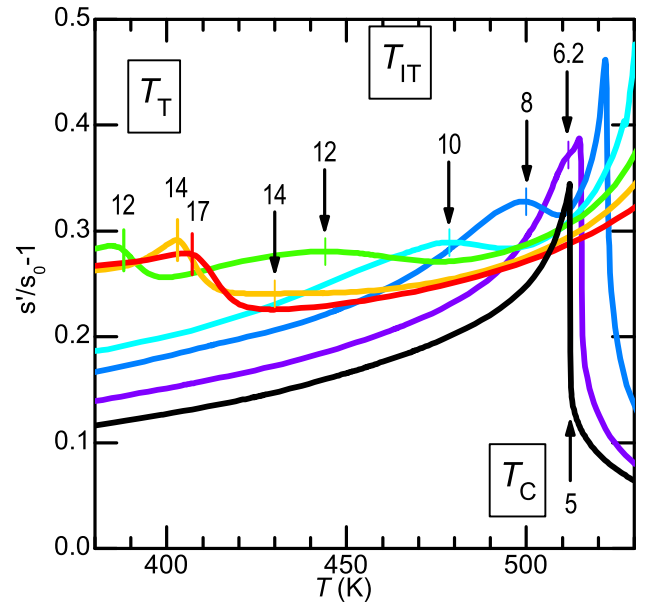


FIG. 4: (Color online) Detail of the anomalies of the elastic compliance at T_{IT} , measured at ~ 1.7 kHz during cooling on samples with $0.05 \leq x \leq 0.17$. The numbers indicate the compositions in %Ti. The curves of 10, 14 and 17% Ti are from Ref. 7.

because χ' and s' are two different response functions of polarization and strain respectively, but, once plotted in the phase diagram, they present an excellent correlation with the MPB determined by diffraction, at least in the middle of the MPB line (see Fig. 7). The dielectric maxima at T_{MPB} are much smaller and broader than the Curie-Weiss peak at T_C (note the logarithmic scale), whereas the anelastic maxima at T_{MPB} have comparable or even larger intensities than the step at T_C (part of the peaked component at T_C has a frequency dispersion denoting relaxation of walls^{7,18}).

At $x = 0.40$ there is no peak attributable to the MPB, but only a minor step below T_T , which is indicated with triangles up to $x = 0.452$; beyond that composition, the step at T_T either disappears or is masked by the MPB peak. The other shallow anomaly centered at ~ 360 K in the curves up to $x \leq 0.465$ is the counterpart of the domain wall relaxation appearing in the losses mentioned above and will be ignored. For $x \geq 0.45$ the peak at the MPB shifts to lower temperature and develops its maximum amplitude at 0.465, which has been argued to correspond to the point of the phase diagram where the anisotropy of the free energy is minimum.⁷ The presence of a peak in s' at the MPB has also been argued to be evidence that the phase transition occurring at the MPB consists mainly in the rotation of the polarization, from the [001] direction of the T phase toward the [111] direction of the R phase. In fact, in that case the transverse (perpendicular to the original [001] direction) component of \mathbf{P} acts as order parameter and is almost linearly coupled to a shear strain, inducing a peaked response also in

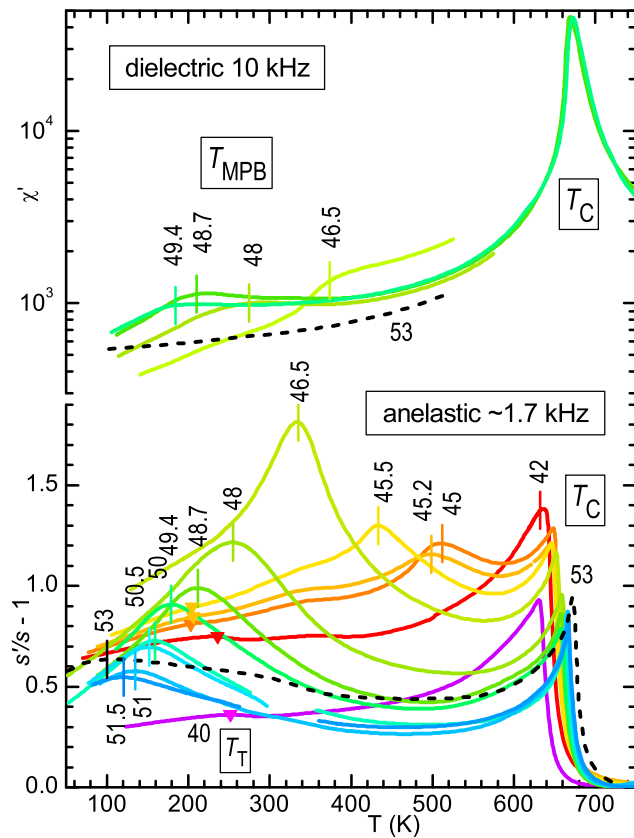


FIG. 5: (Color online) Dielectric susceptibility and elastic compliance measured during cooling on PZT at the compositions indicated besides the curves in % Ti. The T_{MPB} 's are indicated with vertical bars and T_{T} by triangles (only for $40 \leq x \leq 45.2$). Present work: 40, 48.7 and 49.4% Ti; the other curves are from Refs. 7 and 18.

the elastic susceptibility.^{7,18} This would be an evidence that a monoclinic phase, and not only nanotwinned R and T phases, exists below the MPB. Yet, the smooth shape of the maximum is compatible with an inhomogeneous M phase coexisting and possibly promoted by nanotwinning.⁷ In fact, indications continue to accumulate of intrinsic phase heterogeneity near the MPB compositions also on single crystals.²⁹

Beyond $x > 0.465$, the peak at T_{MPB} gradually decreases its amplitude and temperature, and, thanks to the great number of closely spaced compositions, is clearly recognizable as the signature of the MPB up to $x = 0.515$. The next composition, $x = 0.53$ (dashed curves), still has a shallow maximum at a temperature that prosecutes the $T_{\text{MPB}}(x)$ line, but its nature appears different. In fact, the dielectric χ' at the same composition lacks any sign of a maximum, and the overall s' curve does not any more prosecute the trend of the preceding curves. For this reason, the temperature of this maximum at $x = 0.53$ is reported in the phase diagram as T_{MPB} but accompanied by a question mark. A T_{MPB} is extracted also from the curve at $x = 0.42$, even though a separate maximum is not present. It is however the only

composition where s' has no sharp feature at T_{C} , and we assume that this is due to a rounded peak at T_{MPB} very close to T_{C} .

D. Tilt transition near the MPB

The best signatures of the tilt transition below T_{T} are found in the anelastic losses. Figure 6 shows the $Q^{-1}(T)$ curves at all the compositions $x \geq 0.40$ we tested so far (only 45.2%Ti is omitted in order to not overcrowd the figure).

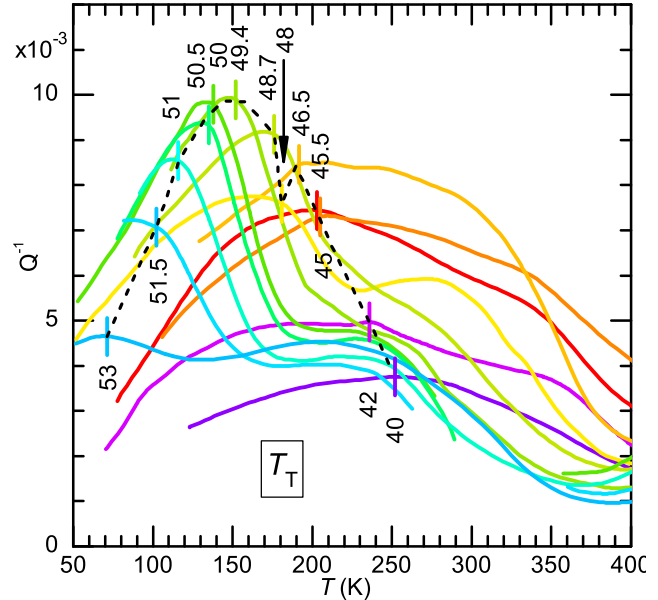


FIG. 6: (Color online) Elastic energy loss coefficient of PZT at the compositions indicated by the numbers (in %Ti), measured during cooling at ~ 1.7 kHz. The anomalies at T_{T} are indicated by vertical bars and joined with a dashed line. Present work: 40, 48.7 and 49.4% Ti; the other curves are from Refs. 7 and 18.

The T_{T} 's up to $x = 0.455$ are the same as deduced from the step in the real part and indicated by triangles in Fig. 5. Up to $x = 0.465$ T_{T} is identified with the temperature of a spike in $Q^{-1}(T)$, which gradually becomes a cusp and starting from $x = 0.48$ becomes a large step. As in the previous figures, the T_{T} 's are marked by vertical bars centered on the curves and joined by a dashed line, in order to better follow the evolution of the anomaly. The transition between the spike/cusp and the step anomaly is unexpectedly sudden, since it occurs within $0.465 < x < 0.48$. Such a discontinuity appears also in the dashed line joining the tilt anomalies, and is marked by an arrow. We emphasize again that the losses generally have a limited reproducibility, because depend on the status of domain walls and defects; therefore, the regularity of the dashed curve joining the tilt anomalies of so many different samples is remarkable and testifies the good and uniform quality of the samples.

IV. DISCUSSION

We refer to the phase diagram of PZT in Fig. 7. Below T_C and with decreasing Ti content, one finds the following phases:^{13,30,31} ferroelectric (FE) tetragonal (T) $P4mm$ with polarization \mathbf{P} along $[001]$, monoclinic (M) Cm with \mathbf{P} rotated toward $\langle 111 \rangle$, rhombohedral (R) $R3m$ with $\mathbf{P} \parallel \langle 111 \rangle$ and antiferroelectric (AFE) orthorhombic (O) $Pbam$ with staggered cations shifts along $\langle 110 \rangle$ and $a^-a^-c^0$ tilt pattern. Below T_T octahedral tilting occurs in all phases.

In Fig. 7, the solid lines join the transition temperatures deduced from our anelastic spectra measured during heating (filled triangles pointing upward), which are generally very close to the points deduced from the dielectric curves (empty triangles). The temperatures measured during cooling are also shown as triangles pointing downward. The figure contains all the data presented here and in Refs. 7,18 and, for completeness, also points obtained at compositions $x \leq 0.05$, that will be discussed in a future paper.

The dashed lines are from the most widely published version of Jaffe, Cook and Jaffe³ with modifications of Noheda *et al.*⁸ around the MPB. In a different version³² the T_{MPB} line below $x = 0.45$ does not prosecute straight up to join T_C almost perpendicularly, but rapidly decreases its slope and joins T_C at $x \sim 0.3$. At present we have indication of a much smaller deviation of T_{MPB} from the datum at $x = 0.42$ (Fig. 5), but already at $x = 0.4$ there is no trace of a double transition.

A. The octahedral tilt instability

The tendency of the BO_6 octahedra in $A^{2+}B^{4+}O_3$ perovskites to tilt has been widely studied and can be rationalized in terms of mismatch between a softer sublattice of longer A-O bonds that compresses a stiffer sublattice of shorter B-O bonds, until the incompressible octahedra tilt in order to accommodate a reduction of the cell and cuboctahedral volume V_A without reducing their volume V_B . In the majority of cases the A-O bonds are softer than the B-O bonds, because they are longer and the cation A shares its valence with 12 nearest neighbors O atoms while B with only 6 of them.¹⁴

This effect is quantitatively expressed in terms of the Goldschmidt tolerance factor

$$t = \frac{\overline{A-O}}{\sqrt{2}B-O} \simeq \frac{r_A + r_O}{\sqrt{2}(r_B + r_O)}$$

which is 1 for the cubic untilted case. In order to predict a tendency to form a tilted phase, t is written in terms of the ideal ionic radii r_X of the appropriate valence and coordination, which are tabulated.³³ If $t < 1$ then the equilibrium B-O bond lengths are too long to fit in a cubic frame of A-O bonds, and tilting occurs below some threshold value; for example, many Sr/Ba

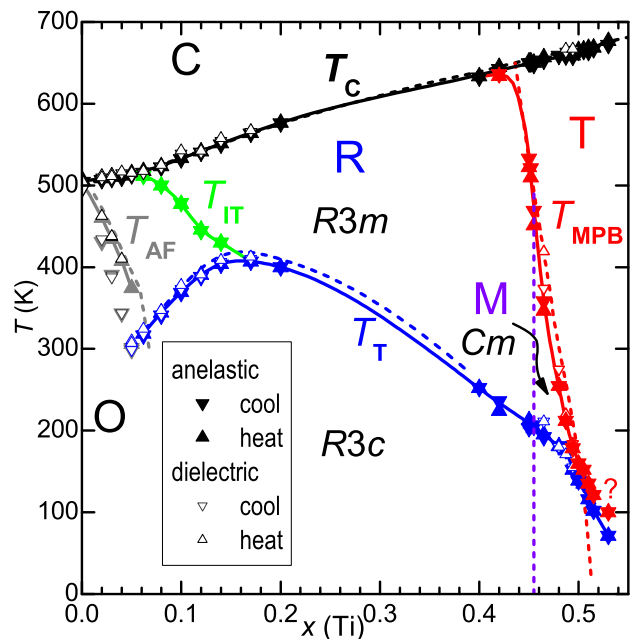


FIG. 7: (Color online) Phase diagram of PZT based on our anelastic and dielectric spectra. The solid lines join the anelastic data measured during heating; the dashed lines are those from Jaffe and Noheda. The question mark reminds that the shallow maximum of s' with $x = 0.53$ at that temperature probably does not signal the MPB crossing.

based perovskites are tilted when $t < 0.985$ at room temperature.¹² Alternatively, the polyhedral volume ratio V_A/V_B is defined,³⁴ which is 5 for the untilted case and becomes < 5 upon tilting. Of all the normal modes of a cubic perovskite, those that induce a decrease of V_A/V_B are the combinations of rigid rotations of the octahedra about the cubic axes, while all other normal modes involve distortions of the polyhedra with little or no change in their volumes.³⁵ Rotations with all the octahedra in phase along the axis are labeled M_3 , because the staggered shifts of the O atoms create a modulation with vector $\frac{1}{2}\langle 110 \rangle$, the M point of the Brillouin zone, while rotations with successive octahedra in antiphase along the axis are labeled R_4 , because the modulation is $\frac{1}{2}\langle 111 \rangle$, the R point of the Brillouin zone.³⁶ These modes are also called antiferrodistortive (AFD), because of the staggered modulation of the atomic displacements, and do not cause the formation of electric dipoles. Most of the low temperature structures of perovskites can be described in terms of combinations of these rotations together with polar modes (shifts of the cations against the O anions). In particular, the low-temperature $R3c$ rhombohedral phase of PZT, is obtained from the high temperature $R3m$ ferroelectric R phase, by applying anti-phase rotations of the same angle about all three pseudocubic axes ($a^-a^-a^-$ in Glazer's notation¹⁶), while the O-AFE structure $Pbam$ of $PbZrO_3$ is a combination of staggered and hence AFE displacements of the Pb^{2+} and Zr^{4+} ions along $[110]$, with anti-phase tilts along $[100]$ and $[010]$

$(a^- a^- c^0)$.

In spite of the considerable amount of research on the phase diagram of PZT, little use has been done of these concepts in order to interpret it. An indication that the mechanism governing tilting in PZT is indeed the A-O/B-O mismatch is the observation that the substitution of 6% Pb^{2+} with the smaller Sr^{2+} induces tilting in an originally untilted T phase of PZT, while when codoping with Sr^{2+} and Ba^{2+} , the latter larger than Pb^{2+} , the opposite effects of the two dopants on the average tolerance factor cancel with each other and no tilting is found.³⁷ When the tilt boundary T_T has been discussed in terms of t , the incongruence of the deep depression near the border with the O-AFE phase has been pointed out,¹³ and explained in terms of frustration of AFE displacements of the Pb ions perpendicularly to the average FE direction $\langle 111 \rangle$. Such displacements lack the long range order of the AFE-O structure, and their frustration would be transmitted to the octahedral tilting through the Pb-O bonds, so lowering the T_T border in proximity with the AFE-O phase.¹³ Certainly the sharp depression in the border to the long range ordering of tilts, the $T_{AF} + T_T$ line, appears to be caused by some frustration, since it is a typical feature of the phase diagrams with competing states,^{38,39} and both the FE/AFE polar modes and different tilt patterns may be in competition.

Let us first consider the AFE/FE competition. The disordered displacements of Pb away from the average polarization have been proposed to occur over the whole R region of the phase diagram and particularly near the other MPB with the T phase, based on the large anisotropic displacement ellipsoids of Pb in Rietveld refinements according to the R structure⁴⁰ or to the co-existence of M and R structures.^{23,30} While in these cases the Pb displacements off-axis with respect to the $\langle 111 \rangle$ direction may be imagined as having a FE correlation leading to a rotation of the polarization away from $\langle 111 \rangle$, recently a soft mode corresponding to AFE Pb displacements has been found near the MPB of PZT and in relaxor PMN and PZN-PT, suggesting that the AFE-like instability is a common feature of nanoscale domain structures of rhombohedral or pseudorhombohedral lead-based perovskites.⁴¹ Considering that such displacements occur over the whole R region or particularly at the MPBs with the O and the T phases, if they are so strongly coupled with the tilts, one would expect a depression of T_T also near the MPB with the T phase, which is not observed. There are some possible explanations for the different behavior of T_T at the two MPBs. One is that the polar displacements away from $\langle 111 \rangle$ might become static and with larger amplitude and AFE correlation only near the AFE border, so causing the frustration between FE and AFE patterns, while at the MPB to the T-FE phase the AFE correlations remain at the stage of an anomalous phonon softening.

On the other hand, it is possible that the main competition occurs between the two different tilt patterns in the R and O phases, since the approaching of the tilt insta-

bility to the FE one indicates that in the $x \rightarrow 0$ region of the phase diagram polar and tilt modes have comparable energetics. It is not evident, however, how the competition between $a^- a^- c^0$ and $a^- a^- a^-$ tilt patterns would cause frustration, since they can transform into each other just by switching on and off the anti-phase tilt about the pseudocubic axis $[001]$. We believe that so strong a depression of the $T_{AF} + T_T$ lines is possible because partial tilting has already occurred at T_{IT} .

B. The intermediate tilt instability $T_{IT}(x)$ line

Before discussing the nature of the instability at T_{IT} , we emphasize the reasons why a positive step of the compliance during cooling like that at T_{IT} should indicate a phase transition and not some kinetic effect related to domain walls or defects: *i*) cooling causes pinning or freezing of domain walls and therefore decreases the susceptibility, while an increase is observed at T_{IT} ; *ii*) in the absence of tilting, the only conceivable walls just below T_C would be between the R-FE domains; if some anomaly in their behavior occurred around T_{IT} , it would appear also, or mainly, in the dielectric susceptibility; *iii*) the shape of the anomaly is independent of the temperature rate, history and frequency,⁷ and therefore is an intrinsic lattice effect.

The T_{IT} line appears as the prosecution of the T_T one toward the lowest x , or equivalently lowest t , and highest temperature, and hence it has been identified as the onset of precursor tilting.⁷ Presumably, between T_{IT} and T_T tilting would be disordered due to the enhanced disorder in the O-Pb-O network near the AFE border, as suggested above.¹³ The drastic depression of T_T would then be due to the fact that most of the mismatch between the Pb-O and (Zr/Ti)-O sublattices is relieved at T_{IT} , and the final transition to a tilted phase with long range order requires the buildup of sufficient elastic energy in the disordered sublattice of tilted octahedra, that it is convenient to switch to the long range ordered phase. This is not alternative to the above discussion on the sharp minimum of $T_{AF} + T_T$ in terms of competing phases. It is simply assumed that the frustration hinders tilting from reaching long range order but not from occurring on the local scale.

This interpretation has not yet been corroborated by a structural study where the onset of tilting below T_{IT} is actually observed and the tilt pattern is established. Actually, superlattice spots in electron diffraction have been interpreted in terms of in-phase M_3 -type tilts within the otherwise $R3m$ phase up to $x \sim 0.15$.^{42,43} That region roughly corresponds to the region delimited by the T_{IT} border, though a border was not seen.^{42,43} These in-phase tilts could not be confirmed by x-ray or neutron diffraction and considerable debate ensued over the interpretation of the electron diffraction $\frac{1}{2} \langle 110 \rangle$ spots in terms of AFE $\langle 110 \rangle$ Pb displacements rather than M_3 -type tilts, due to the much weaker strength of the latter

and the greater sensitivity of electron diffraction to the damaged surface.^{13,44}

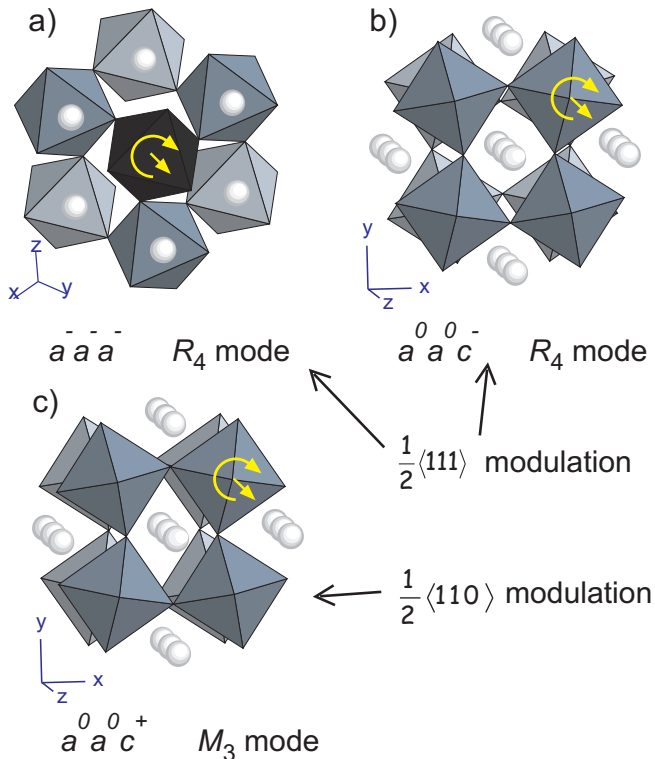


FIG. 8: Three tilt patterns of the BO₆ octahedra. The O ions at the vertices of the octahedra and the B ions at their centers are not shown; the A ions are white. The darker octahedra are in planes closer to the observer. a) $a^- a^- a^-$ tilt pattern of the *R*_{3c} structure seen from a direction close to the $\langle 111 \rangle$ rotation axis; b) out of phase and c) in phase rotation about the $[001]$ direction. In b) and c) the octahedra of different planes share only O atoms that do not move under tilting..

The *M*₃ tilts are in the first place in the search for a mechanism behind the phase transformation at T_{IT} , because they would cause weak superlattice peaks at positions coinciding with those from the disordered AFE Pb displacements, so explaining why their onset below T_{IT} has not yet been noticed. In fact, the disorder in the Pb sublattice, including AFE-like shifts, survives even in the cubic phase, as demonstrated by the observation of electron diffraction $\frac{1}{2} \langle 110 \rangle$ spots^{42,43} and the fact that EXAFS probes the same local environment of Pb⁴⁵ and Zr/Ti,⁴⁶ both in the FE and in the cubic phases. It seems reasonable to assume that the AFE cation displacements develop their short range order together with the FE order below T_C , so producing superlattice peaks of the $\frac{1}{2} \langle 110 \rangle$ type, that mask those from subsequent octahedral tilting below T_{IT} , if this is of *M*₃ type. The difficulty with the last assumption is that the final tilting below T_T is of *R*₄ type, and the *M*₃ in-phase tilting is an instability of different type rather than a precursor to it.

C. $\frac{1}{2} \langle 110 \rangle$ reflections from hindered $\frac{1}{2} \langle 111 \rangle$ modulation of the tilts?

In order to reconcile the observation of *M*-type modulation below T_{IT} with an expected short range *R*-type modulation, we assume that the propagation of tilt fluctuations is hindered by the lattice disorder associated with Ti substituting Zr, with the consequent frustration of the Pb displacements, and possibly other defects. Therefore, rather than to consider fluctuations of infinitely extended normal modes, it is more appropriate to consider the fluctuations of small clusters of octahedra, whose size is limited by the local disorder. This makes the different types of tilting represented in Fig. 8 inequivalent, since they have different correlation volumes. In a first approximation consider a network of rigid octahedra, that, in order to comply with the mismatch with the Pb-O network, can only tilt without distortions. This is the so-called rigid unit model, whose implications on the anisotropy of the phonon dispersions has been analyzed.⁴⁷ Here we focus on the effects that the anisotropy of the correlation length might have on the diffraction patterns.

Consider first the rotation of a single octahedron about one of the cubic axes ($[001]$ in Fig. 8b) or c)); this will cause a rotation of all the other octahedra in the same plane perpendicular to the axis in an AFD fashion, creating a $\frac{1}{2} \langle 110 \rangle$ modulation, with a correlation length l_{\perp} , perpendicular to the rotation axis, which is an increasing function of the B-O bond strength. In the pure rigid unit model l_{\perp} is infinite and there is no correlation at all with the other planes of octahedra, because they share corners of the tilting octahedra only through immobile O atoms. In practice there is an interaction with the adjacent planes through the less energetic B-O-B bond bending and the extensions of the longer and weaker A-O bonds, resulting in a finite correlation length l_{\parallel} along the rotation axis, however shorter than l_{\perp} . This means that the correlation volume surrounding an octahedron tilting about a $\langle 100 \rangle$ direction is a flat disc of diameter $2l_{\perp}$ and thickness $2l_{\parallel}$ with $l_{\parallel} \ll l_{\perp}$, and this will create superlattice reflections more intense and sharp at $\frac{1}{2} \langle 110 \rangle$ than at $\frac{1}{2} \langle 111 \rangle$. On the other hand, the rotation of an octahedron about a $\langle 111 \rangle$ axis (Fig. 8a)), as the soft *R*₄ mode in the *R*_{3c} structure, will affect all the surrounding octahedra, which share shifted O atoms both above and below the $[111]$ plane containing the rotating octahedron. Therefore, for an octahedron rotating about a $\langle 111 \rangle$ axis the correlation volume is a sphere with diameter $2l_{\perp}$, containing more octahedra than in the previous case. We therefore postulate that below T_{IT} the magnitudes of the tilts start becoming so large to cause their propagation through the correlation volume, as for any tilt instability, but this will occur first for those clusters where a deviation toward $\langle 100 \rangle$ tilt, with smaller correlation volume, is favored by the local cation disorder. In this first stage between T_{IT} and T_T , only $\frac{1}{2} \langle 110 \rangle$ superlattice peaks would appear, easily masked by those from

AFE cation correlations. On further cooling below T_T , the increased instability of the R_4 mode and long range elastic interactions trigger the long range tilt order of the $R3c$ phase. In other words, in the absence of disorder or frustration T_T and T_{IT} would coincide and represent the temperature below which the propagation of the $a^-a^-a^-$ tilt instability starts. In the presence of disorder, local tilting about $\langle 100 \rangle$ axes is favored because of its smaller correlation volume; the resulting disordered tilting partially relieves the mismatch between Pb-O and (Zr/Ti)-O bonds, and further cooling below T_T is necessary in order to reach the long range $a^-a^-a^-$ ground state. This may explain the deep depression of T_T below $x < 0.15$.

D. The kink in the tilt instability $T_{IT}(x)$ line and the effect of coupling of different modes on the phase diagram

If octahedral tilts and polar modes were independent of each other, the T_C and $T_T + T_{IT}$ lines might approach and possibly cross each other in an independent manner. Instead, T_{IT} merges with T_C at $x = 0.06$ with a noticeable kink around $x \sim 0.1$. The T_{IT} line seems "attracted" by T_C , as if the tilt instability were favored by the ferroelectric one. On the other hand, also T_C may feel some effect from the proximity with T_{IT} , since its slope slightly decreases after joining with T_{IT} below $x \sim 0.05$. It appears that both T_{IT} and T_C increase with respect to the trend extrapolated from higher x , when they are far from each other. This is shown in Fig. 9, where the dashed lines are the extrapolations (with no pretension of quantitative analysis) of T_C and T_T . The vertical arrows are the maximum deviations of the actual T_C and T_{IT} lines from their extrapolations, $\Delta T_C \sim 16$ K and $\Delta T_T \sim 48$ K. A possible qualitative explanation of this observations is in terms of cooperation between a stronger FE instability and a weaker AFD tilt instability. The FE mode leaves the lattice unstable also below T_C , since its restiffening is gradual, and also affects the modes coupled to it, in particular favoring the condensation of modes cooperatively coupled to it at a temperature higher than in the normal stiff lattice away from T_C . The rotations of the octahedra are certainly coupled with the polar modes, as demonstrated by the polarization^{48,49} and dielectric^{7,50} anomalies at the tilt transitions, and the issue whether this coupling is cooperative or competitive is discussed in Sect. IV H. Assuming that the first eventuality is true, one has a mechanism that enhances T_{IT} in the proximity of T_C , but the coupling works also in the other sense: the proximity of the tilt instability favors the condensation of the FE mode, enhancing T_C . The energies involved in the FE instability are larger than those involved in tilting, as indicated by the fact that $T_C > T_T$, and accordingly the perturbation of the FE mode on the tilt mode is larger: $\Delta T_T \sim 3\Delta T_C$. A phenomenological model⁶⁰ that may be applied to explain these effects will be described in Sect. IV G.

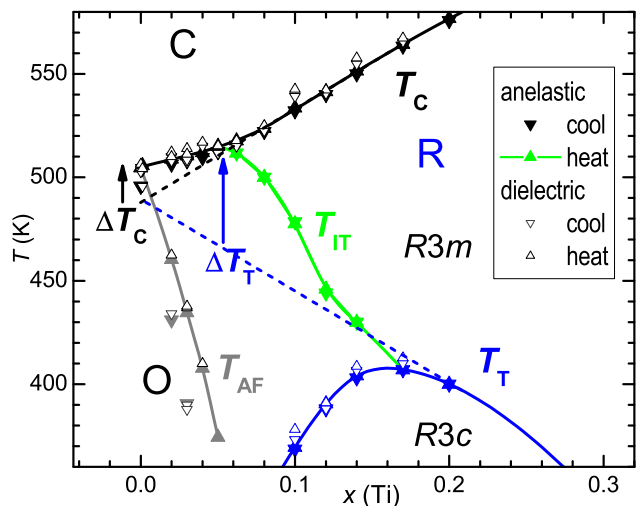


FIG. 9: (Color online) Zr-rich region of the phase diagram based on our anelastic and dielectric spectra. The dashed lines are extrapolations from the high- x behavior of $T_C(x)$ and $T_T(x)$. The arrows ΔT_C and ΔT_T represent the deviation from the extrapolated behavior.

E. Kinks in the T_{MPB} and T_T lines

Other new features of the PZT phase diagram that derive from the present data are the approaches of the $T_{MPB}(x)$ line with T_T and T_C , and a distinct kink in T_T when encounters T_{MPB} . This is better seen in the detail of the MPB region in Fig. 10, where, besides the same data of Fig. 7, other points of T_{MPB} and T_T are reported from the literature. The data are from diffraction⁸ (\diamond) piezoelectric coefficient⁵¹ d_{11} (\square), $1/s_{11}$ measured with piezoelectric resonance⁵² (\circ), Raman⁹ ($-$), dielectric ($+$) and infrared (\times)²¹ spectroscopies.

Let us first consider how $T_T(x)$ enters the MPB region. The points from the literature, obtained from different techniques and samples, are rather sparse, but those from our anelastic and dielectric spectra have little dispersion, and show a clear change of slope of $T_T(x)$ when it approaches T_{MPB} at $0.487 < x < 0.494$. This narrow composition range is close to but not the same over which the anomaly in Q^{-1} changes between cusped and step-like (Fig. 6). In fact that change, marked by arrows in Fig. 10, occurs at $x \lesssim 0.48$, and therefore the two changes may depend on different mechanisms. We will discuss the transition in the shape of the Q^{-1} anomaly in Sect. IV I, and now we focus on the kink in the T_T line, which we think is closely connected with the proximity to the MPB.

Also our T_{MPB} points draw a curve with little dispersion, compared to the body of data in the literature, but in this case a difference emerges in the low temperature region: even though with only three points below 100 K, the data from diffraction⁸ and Raman⁹ define an almost straight MPB border that ends at $T = 0$ at

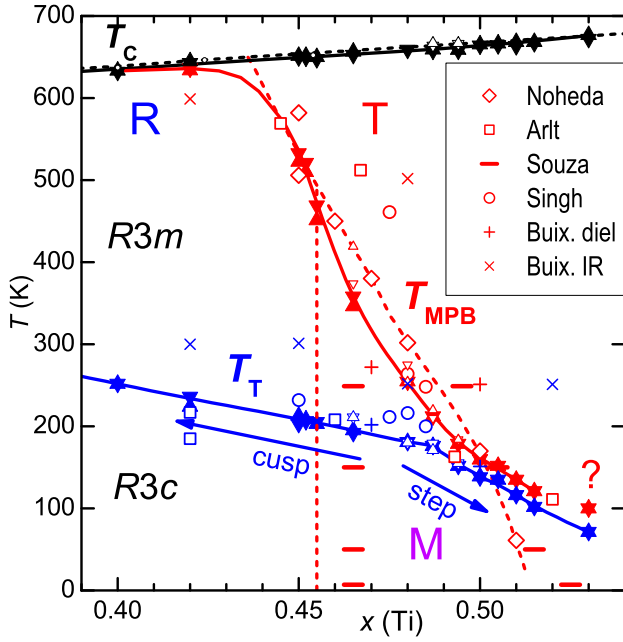


FIG. 10: (Color online) Enlargement of the MPB region of the phase diagram of PZT. Triangles and solid lines from our measurements, as in Fig. 7. Dashed lines and diamonds from Noheda and other open symbols as indicated in the legend. The shape of the continuous $T_{\text{MPB}}(x)$ line between $x = 0.42$ and 0.45 is hypothetical.

$x = 0.520 \pm 0.005$. Instead, our data define a curved line that never crosses T_{T} . Our closely spaced points in the phase diagram and the regular evolution of the spectra from which they are obtained (Figs. 5 and 6) suggest that the effect is real and characteristic of good quality ceramic samples. The last point with the question mark, obtained from the dashed curve in Fig. 5, probably does not correspond to T_{MPB} , but the difference remains at $x = 0.515$ between our curve at 120 K, and two points at 50 – 60 K from diffraction and Raman scattering. These discrepancies may depend on differences in the samples rather than on the experimental technique. In fact, the existence of the intermediate monoclinic phase and its nature are not yet unanimously accepted, and it is also proposed that, besides nanoscale twinning, defect structures like planes of O vacancies may have a role in defining the microstructure of PZT and act as nuclei for intermediate phases.⁵³ Hence, there is a range of microstructures that may well reflect in the position of the MPB, but, again, the consistency and regularity of the data encourage to consider the features presented here as intrinsic of the PZT phase diagram and not vagaries from uncontrolled defects.

It results that also T_{T} and T_{MPB} almost coincide over an extended composition range, with T_{MPB} seemingly pushed up by T_{T} . For $x > 0.49$, T_{MPB} deduced from the maximum in s' and T_{T} deduced from the step in Q^{-1} run parallel and close to each other and it is difficult to assess whether they still represent two distinct

transitions or instead they are the manifestations of a same combined polar and tilt transition.

F. Merging of tilt and polar instabilities also in NBT-BT

Another example in which tilt instability lines merge with polar instability lines is $(\text{Na}_{1/2}\text{Bi}_{1/2})_{1-x}\text{Ba}_x\text{TiO}_3$ (NBT-BT).⁵⁴ This system has much stronger chemical disorder than PZT and a more complicated and less defined phase diagram, especially beyond the MPB composition x (Ba) > 0.06 , where the correlation lengths are so short to render the material almost a relaxor. In Fig. 11 the phase diagram of NBT-BT is presented together with that of PZT. The broken lines represent the borders between regions with different tilts, while the solid lines are polar instabilities (T_{AF} in PZT is both tilt and polar). The regions where two types of instabilities merge are vertically hatched, while differently slanted hatches represent different tilt patterns. In NBT the tolerance factor is small due to the smallness of the mean A ion size of Na^+ and Bi^{3+} combined, and is increased by substituting with Ba. Tilting occurs in two stages, first $a^0a^0c^+$ (T phase) below T_1 and then $a^-a^-a^-$ (R) below T_2 , and both T_1 and $T_2 + T_{\text{MPB}}$ have negative dT/dx , so enclosing the low temperature/low tolerance factor region of the phase diagram, as discussed in Sect. IV A (the T_1 line actually disappears into a highly disordered relaxor-like region). At variance with PZT, the polar instabilities occur at temperatures lower than those of tilting, and in two stages: first an almost AFE or ferroelectric region below a temperature T_m signaled by a maximum in the dielectric susceptibility, and then FE below the so-called depolarization temperature T_d . The intermediate \sim AFE structure is due to shifts of the Ti and Bi cation along [001] in opposite directions, so to make P almost null, and therefore is not the result of coupling with the AFD $a^0a^0b^+$ tilting.⁵⁵ The FE phase, however, appears below a $T_d < T_2$ at $x = 0$, which rises and merges with the decreasing $T_2(x)$ at $x = 0.02$ ⁵⁴ or 0.03 .⁵⁶ Beyond 6% Ba, the T_d and $T_2 \equiv T_{\text{MPB}}$, the latter ill defined, separate again. As a result, the border T_d to the FE phase, instead of simply crossing T_2 , merges with it in the range $0.02 < x < 0.06$, following a wavy path. This would not be the only instance in the NBT-BT phase diagram where the tilt modes trigger a mixed tilt-polar transition, since it has been recognized that in pure NBT both the transitions at T_1 and T_2 are of such a type.⁵⁷

Similarly to the cases of $T_{\text{IT}}/T_{\text{C}}$ and $T_{\text{C}}/T_{\text{MPB}}$ in PZT, the coincidence of T_d and T_2 in the composition range $0.02 < x$ (Ba) < 0.06 may be interpreted as a manifestation of cooperative coupling between tilt and FE instabilities. Interestingly, like Pb^{2+} also Bi^{3+} has a lone pair electronic configuration, with the tendency to reduce its coordination number and form short bonds with covalent character^{55,58} which couple tilt and polar modes.⁵⁹

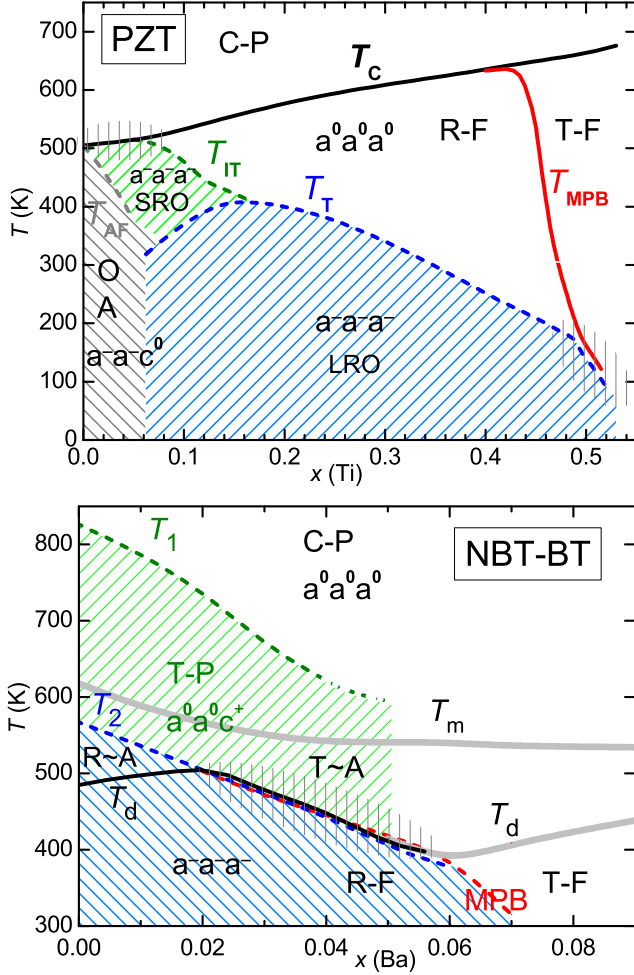


FIG. 11: (Color online) Phase diagrams of PZT and NBT-BT,⁵⁴ where the broken lines are tilt instability borders, while the solid lines are polar instability borders. Vertical hatching evidences the regions where the two types of lines merge. Differently slanted patterns represent different tilt patterns. P, F and A stand for paraelectric, ferroelectric and antiferroelectric; SRO and LRO stand for short/long range order.

G. Merging of tilt and polar instabilities seen as trigger type transitions

A possible mechanism for the merging of two transitions with order parameters (OPs) of different symmetries had been proposed by Holakowsky⁶⁰ and carried on by Ishibashi;⁶¹ This is also the case of octahedral tilting, whose OP is the rotation angle ω , and polar or antipolar modes with OP P (all one-dimensional for simplicity). Holakowski⁶⁰ treated the case of a FE transition triggered by another OP, and we will adapt his arguments to a tilt transition triggered by the FE instability, referring to T_{IT} . In this case the minimal Landau expansion of the free energy is

$$F = \frac{a}{2}P^2 + \frac{b}{4}P^4 + \frac{a_\omega}{2}\omega^2 + \frac{b_\omega}{2}\omega^4 + \frac{c_\omega}{6}\omega^6 + F_c \quad (1)$$

where $a = \alpha(T - T_C)$ and $a_\omega = \alpha_\omega(T - T_\omega)$ represent the soft modes ideally vanishing at T_C and $T_\omega < T_C$. In the argument, the temperature dependence of a_ω is irrelevant, and Holakowski sets it constant; in our case it should be $\lesssim T_{IT}$. The coupling part F_c contains mixed terms $P^m\omega^n$. Since ω and P have different symmetries, not all the mixed terms are invariant under the allowed symmetry operations in the cubic phase, under which F must be invariant; the lowest order term allowed by symmetry is⁶²

$$F_c = -\frac{\gamma}{2}P^2\omega^2. \quad (2)$$

Such a term is always possible but generally overlooked when mixed terms of lower order prevail. If $\gamma > 0$ this term lowers the free energy when both $P \neq 0$ and $\omega \neq 0$, describing a cooperative polarization-tilting coupling. After solving the equilibrium condition $0 = \partial F / \partial P$, the equilibrium value of ω is expressed in terms of equilibrium P , so that F is written only in terms of P , and F_c renormalizes b as $b' = b - \gamma^2/b_\omega$. The reason why the tilting free energy cannot be truncated to ω^4 is that the renormalized b'_ω can become negative, in which case a positive 6th order term is needed to stabilize the free energy. We refer to the paper of Holakowsky for the details and only report the result adapted to our case. The occurrence of the FE transition promotes tilting through the biquadratic coupling term, resulting in a tilt transition at a temperature T_t that can be also considerably

higher than T_ω (which is zero in Ref. 60). Increasing the magnitude of the coupling constant γ , the onset of the tilt instability is shifted to higher temperature and the following cases are encountered. When $b' > 0$ the tilt transition is second order and occurs at

$$T_t = T_C - \frac{a_\omega b}{\gamma \alpha},$$

hence a temperature higher than T_ω , if $T_\omega \ll T_C$. If $b_0 < b' < 0$ with $b_0 = -4\sqrt{a_\omega c_\omega}/3$ then the transition is first order and occurs between T_t and T_C ; if $b' < b_0$ the free energy may have minima at both $P \neq 0$ and $\omega \neq 0$ (distinct from those of the pure FE phase with $\omega = 0$) already at T_C and therefore a first order transition to a combined tilt/polar transition is possible at $T > T_C$.

The above mechanism only requires that the tilt-polarization coupling is cooperative and enough strong, which is not forbidden by any constraint of symmetry or general principle, and we think that it can be at the basis of the anomalous rise and merging in temperature of the tilt and FE instabilities in Zr-rich PZT. The situation should actually be more complicated, since the triggered transition does not produce a phase with a clear symmetry of the polar and tilt OPs, apparently because the energy shifts from chemical disorder compete with the energies involved in the regular Landau expansion of a homogeneous crystal. This disorder would be responsible for preventing the complete tilt transition with long

range order down to $T_T \ll T_{IT}$, and should somehow be included into in the Landau expansion. These considerations should prevent from applying the above simple formulas for deducing the magnitude of γ from the upward shift of T_{IT} . Yet, an independent indication that γ is indeed large and positive comes from the positive step in the dielectric susceptibility below T_T , as shown in Sect IV H 3.

The possibility should be explored that a similar mechanism accounts for the proximity, instead of crossing, of the T_{MPB} and T_T lines at $x > 0.50$, as we observe in our large grain ceramic samples. In this case, the FE OP might be the transversal component P_t , responsible for the rotation of \mathbf{P} away from the tetragonal axis, and which takes a role in the peak of s' .

The mechanism of the trigger-type transition has been applied so far to very few cases, like $\text{Bi}_4\text{Ti}_3\text{O}_{12}$ ⁶³ and recently proposed to explain the sequence of phase transitions of the multiferroic BiFeO_3 ,⁶⁴ and is therefore considered as very rare.⁶⁴ The possibility that a trigger-type mechanism is also responsible for the particular features of the phase diagrams of PZT and NBT-BT suggests that it may be not so rare.

Finally, T_{MPB} seems to join also T_C smoothly, although the upper end of the T_{MPB} line in the phase diagrams above is based on only one datum and largely hypothetical (but in line with the much more marked effect in Ref. 32). This case is different from the previous ones, since the OP active below T_{MPB} is not independent from that active at T_C , both being the polarization, and a triggered phase transition as above would be meaningless. Nonetheless, the manner in which T_{MPB} meets T_C deserves further investigation.

H. Competition or cooperation of tilt and polar modes?

The interpretation above contrasts with the widespread opinions that the coupling between tilt and polar modes is negligible or competitive, and therefore it is opportune to discuss the nature of the interaction between polar and tilt modes.

1. Negligible tilt-polarization coupling

In the context of the general trends of the perovskite phase diagrams at different compositions, the coupling between tilting and deformation or polar modes has been considered negligible in rhombohedral perovskites.⁶⁵ This assumption was based on the observation that in a large number of rhombohedral perovskites, including FE ones, the rotation angle ω of the octahedra and the polyhedral volume ratio mentioned in Sect. IV A are related by

$$V_A/V_B = 6 \cos^2 \omega - 1, \quad (3)$$

which is valid in the absence of octahedral distortions. In other words, the tilt angles are independent of the distortions,⁶⁵ which necessarily occur in the FE phases. This fact, however, shows that the mismatch between the bond lengths or polyhedral volumes is accommodated almost exclusively by the tilting mechanism, and this is understandable, since the only two normal modes producing a large change of V_A/V_B are in-phase and anti-phase rotations of the octahedra, while all the other modes yield distortions with little change of V_A/V_B .³⁵ Therefore, while the validity of Eq. (3) is a manifestation of the fact that V_A/V_B depends almost exclusively on the tilting angle ω , it does not imply a lack of coupling between tilting and the other distortion and displacement modes, for example influencing the type of tilt correlations.

2. Competitive tilt-polarization coupling

The most widely accepted view is of a competition between FE and AFD instabilities, based on their opposite behavior under pressure.⁶⁶⁻⁶⁹ Indeed, in titanates and other perovskites pressure suppresses FE and promotes tilting, and this can be simplistically understood in terms of a steric mechanism: FE requires more space for cation off-centering while the octahedral rotation is promoted by a compression of the lattice that amplifies the mismatch between B-O and A-O sublattices. These observations, however, show that the two instabilities behave in opposite manner under pressure, but not necessarily that they compete against each other. It should also be noted that there are several exceptions to the "rule" that pressure favors tilting, for example perovskites with trivalent B = Al,⁷⁰ Gd,⁷¹ and there are even studies that assume that the general rule is just the opposite: pressure induces the more symmetric cubic structure.⁷² These different behaviors under pressure depend on the relative compressibilities of the AO_{12} and BO_6 polyhedra, which can be rationalized in terms of the bond valence sum concept.⁷³ It appears that in the zirconates and titanates the BO_6 octahedra are stiffer than the AO_{12} cuboctahedra, which is the usual case when B has larger valence than A.

Another strong and widely accepted⁶⁹ indication of competitive AFD-FE interaction comes from simulations⁷⁴ on SrTiO_3 showing that the FE mode of cation displacements along $\langle 111 \rangle$ and the AFD anti-phase tilt modes compete against each other. The simulations are done on SrTiO_3 , which actually is not ferroelectric due to quantum fluctuations, but their result is clear: neglecting quantum fluctuations, the temperature of the tilt instability is 25% higher if the FE mode is frozen, while T_C is 20% higher if the AFD mode is frozen. This means that the two modes tend to cancel each other rather than cooperate, and the microscopic mechanism is identified in the mutual anharmonic interaction. The behavior of T_C and T_{IT} in PZT or T_d and T_2 in NBT-NT, however, seems the opposite. It is possible that the nature of interaction between AFD and

FE modes is different when the A ion is Pb instead of Sr, since the difference is not only of ionic size but there is also a more strongly covalent character of the bond when Pb goes off center.^{55,58} The other difference between the SrTiO₃ and PZT case is that in the first only the z component of the R_4 mode becomes unstable, leading to a T structure, while in PZT all three components yield the R structure. It is therefore unlikely that the simulation of SrTiO₃ can be plainly generalized to Pb compounds. Rather, it may be more appropriate to refer to similar simulations⁶⁴ on multiferroic BiFeO₃, where also Bi³⁺ has the stereoactive lone pair like Pb²⁺. Such simulations indicate that the sequence of FE and AFD transitions is indeed dominated by the trigger-type mechanism, and that the coupling between the two types of modes is strong and both competitive and cooperative, due to the fact that the order parameters are multicomponent.⁶⁴

3. Cooperative tilt-polarization coupling

That the tilts are coupled with polar modes is demonstrated by the fact that below T_T there is a positive step in the real part of the dielectric susceptibility,^{7,18,43} as clearly shown in Fig. 2, and in the polarization.⁴⁸ If the modes competed against each other, then the onset of tilting should depress rather than enhance the polarization and its derivative, and this becomes clear when considering the biquadratic coupling term, Eq. (2), the leading term allowed by symmetry. Below T_T the equilibrium tilt angle $\bar{\omega}$ starts growing, and F_c renormalizes the term of the free energy $\propto P^2$ as $a' = a - \gamma\bar{\omega}^2$ and hence the dielectric stiffness $\chi^{-1} = \partial^2 F / \partial P^2 \simeq a'$. Therefore, below T_T a positive step is observed in χ if $\gamma > 0$ and a negative one if $\gamma < 0$. From Fig. 2 it appears $\gamma > 0$, namely the coupling between ω and P is cooperative. In principle it would be simple to estimate the magnitude of γ from that of the step in χ' at T_T , the magnitude of $\bar{\omega}$ from diffraction and $a = \alpha(T - T_C)$ from the Curie-Weiss peak. However, as noted in Sect. IV F, the simple free energy (1) does not contain the effect of disorder that depresses T_T , and the relevance of γ deduced in this manner would be questionable.

Additional indications of cooperative tilt-polarization coupling are the fact that the application of an electric field in PZT modified with Sn and Nb enhances T_T of few degrees.⁷⁵ and its prediction in BiFeO₃ from a first-principle simulation.⁶⁴ The coupling between FE and AFD modes has also been discussed in relation with the appearance of new Raman^{76,77} and infra-red²¹ modes below T_T .

We think that the fact that tilt and polar instability lines merge over extended composition ranges instead of crossing each other are due to a cooperative coupling between polar/antipolar and tilt modes. It is interesting to note that a simulation of the PZT phase diagram including tilt degrees of freedom has already been done,¹⁷

and the T_{MPB} line, though finally crosses T_T , presents a marked bend on approaching it, exactly as appears from our anelastic and dielectric experiments.

I. Transition in the shape of the Q^{-1} anomaly at T_T : a possible sign of R/M border

As already noted in Sect. IV E, the kink in the T_T line and the transition in the shape of the Q^{-1} anomaly (Fig. 6) appear at slightly different compositions, suggesting that the latter may have a different origin from the proximity to the MPB and hence polarization-tilt coupling.

If this were the case, the most obvious explanation for the change of the Q^{-1} anomaly would be the postulated border separating R and M phases.^{8,9,17} The existence of this border is one of the yet unsettled issues on the phase diagram of PZT, since there are various diffraction studies, also recent and on single crystals,^{23,30} whose Rietveld refinements strongly suggest that the R and M phases coexist at least down to $x = 0.4$, so excluding a definite phase border. In addition, according to the view that the M phase is actually a nanotwinned R or T phase,^{5,6} this border would not exist. Therefore, a R/M border would be highly significant: it would imply the existence of a long range M phase. A puzzling feature of this border would be its verticality. In fact, a truly vertical phase boundary in the $x - T$ phase diagram would be understandable at a specific composition that allows a phase to be formed with commensurate cation order. This is certainly not the case of the postulated R/M border in PZT, where no Zr/Ti ordering has ever been observed, and anyway $x \simeq 0.47$ is too far from the closest relevant composition $x = \frac{1}{2}$. Indeed, the R/M boundary found by first principles based simulations is not vertical: it starts at a triple point with T_C and T_{MPB} at $x_1 = 0.463$ and ends at $T = 0$ and $x_2 = 0.476$.¹⁷ No experimental evidence exists so far of the crossing of such a border with change of temperature, and the change of the shape of the Q^{-1} anomaly between 0.465 and 0.48 is not a conclusive evidence of its existence, since it might be associated with a change of the character of the transition through polarization-tilt coupling near the MPB. Further experiments at more closely spaced compositions are necessary to ascertain this point.

V. CONCLUSIONS

Anelastic and dielectric measurements are reported at compositions of the phase diagram of $\text{PbZr}_{1-x}\text{Ti}_x\text{O}_3$ near the two morphotropic phase boundaries (MPB) of the rhombohedral phase with the tetragonal and the orthorhombic phases. Several new features are found in both regions, and discussed in terms of octahedral tilting and cooperative coupling between the tilt and polar/antipolar modes.

We confirm the recent discovery⁷ of a new phase transition at a temperature T_{IT} that prosecutes the border T_T of the tilt instability up to the Curie temperature T_C , in the region where T_T drops and meets the border with the orthorhombic antiferroelectric phase. The new phase is assumed to represent the initial stage of octahedral tilting, without long range order due to the enhanced cation disorder near the AFE border. Lacking evidence from diffraction for this intermediate tilt region, the rationale for the assumption that tilting is involved is discussed in terms of mismatch between the networks of Pb-O and (Zr/Ti)-O bonds, as usual for tilted perovskites. In addition, it is proposed that, due to the anisotropy of the correlation length of different types of tilts, the initial stage of tilting in the presence of disorder involves flat clusters of octahedra rotating about $\langle 100 \rangle$ axes, so producing $\frac{1}{2} \langle 110 \rangle$ type modulations, even when the final long range modulation is of $\frac{1}{2} \langle 111 \rangle$ type.

The T_{IT} tilt instability line merges with the ferroelectric T_C with an evident step and both temperatures appear enhanced with respect to the extrapolations from the region where they are far from each other. Also the T_T line presents a clear kink when it meets the MPB and, contrary to previous experiments, T_{MPB} is found to deviate and go parallel or even merge with T_T , instead of

crossing it. These observations of deviations and merging of tilt and polar instability borders are compared to a similar example in NBT-BT, and explained in terms of strong and cooperative interaction between the polar and the tilt modes, which causes a trigger type transition. Since the prevalent opinions are that tilt-polarization coupling is competitive or negligible, and the trigger-type transitions are extremely rare, the various indications of polar-tilt coupling in PZT are reviewed and discussed.

Another feature that is considered is a rather abrupt transition in the shape of the anomaly in the elastic losses at T_T . The anomaly is a peak or cusp for $x \leq 0.465$ and a step for $x \geq 0.48$. The possibility is discussed that between these two compositions there is an actual border between rhombohedral and monoclinic phases.

Acknowledgments

The authors thank Mr. C. Capiani (ISTEC) for the skillful preparation of the samples, Mr. P.M. Latino (ISC) and A. Morbidini (INAF) for their technical assistance in the anelastic and dielectric experiments.

-
- ¹ E. Sawaguchi, J. Phys. Soc. Jpn. **8**, 615 (1953).
² H. Jaffe, Proc. IEE, B Electron. Commun. Eng. UK **109**, 351 (1962).
³ B. Jaffe, W.R. Cook and H. Jaffe, *Piezoelectric Ceramics*. (Academic Press, London, 1971).
⁴ B. Noheda, D.E. Cox, G. Shirane, L.E. Cross and S.-E. Park, Appl. Phys. Lett. **74**, 2059 (1999).
⁵ A.G. Khachatryan, Phil. Mag. **90**, 37 (2010).
⁶ K.A. Schönau, L.A. Schmitt, M. Knapp, H. Fuess, R.-A. Eichel, H. Kungl and M.J. Hoffmann, Phys. Rev. B **75**, 184117 (2007).
⁷ F. Cordero, F. Trequattrini, F. Craciun and C. Galassi, J. Phys.: Condens. Matter **23**, 415901 (2011).
⁸ B. Noheda, D.E. Cox, G. Shirane, R. Guo, B. Jones and L.E. Cross, Phys. Rev. B **63**, 014103 (2000).
⁹ A.G. Souza Filho, K.C.V. Lima, A.P. Ayala, I. Guedes, P.T.C. Freire, F.E.A. Melo, J. Mendes Filho, E.B. Araújo and J.A. Eiras, Phys. Rev. B **66**, 132107 (2002).
¹⁰ H.D. Megaw, Proc. Royal Soc. **58**, 133 (1946).
¹¹ P.M. Woodward, Acta Cryst. B **53**, 44 (1997).
¹² I.M. Reaney, E.L. Colla and N. Setter, Jpn. J. Appl. Phys. **33**, 3984 (1994).
¹³ D.I. Woodward, J. Knudsen and I.M. Reaney, Phys. Rev. B **72**, 104110 (2005).
¹⁴ I.D. Brown, Acta Cryst. B **48**, 553 (1992).
¹⁵ I.D. Brown, A. Dabkowski and A.A. McCleary, Acta Cryst. B **53**, 750 (1997).
¹⁶ A.M. Glazer, Acta Cryst. B **28**, 3384 (1972).
¹⁷ I.A. Kornev, L. Bellaiche, P.-E. Janolin, B. Dkhil and E. Suard, Phys. Rev. Lett. **97**, 157601 (2006).
¹⁸ F. Cordero, F. Craciun and C. Galassi, Phys. Rev. Lett. **98**, 255701 (2007).
¹⁹ M. Hinterstein, K.A. Schoenau, J. Kling, H. Fuess, M. Knapp, H. Kungl and M.J. Hoffmann, J. Appl. Phys. **108**, 024110 (2010).
²⁰ M. Deluca, H. Fukumura, N. Tonari, C. Capiani, N. Haseike, K. Kisoda, C. Galassi and H. Harima, J. Raman Spectr. **42**, 488 (2011).
²¹ E. Buixaderas, D. Nuzhnyy, J. Petzelt, L. Jin and D. Damjanovic, Phys. Rev. B **84**, 184302 (2011).
²² R. Ranjan, A.K. Singh, Ragini and D. Pandey, Phys. Rev. B **71**, 092101 (2005).
²³ D. Phelan, X. Long, Y. Xie, Z.-G. Ye, A.M. Glazer, H. Yokota, P.A. Thomas and P.M. Gehring, Phys. Rev. Lett. **105**, 207601 (2010).
²⁴ R. Singh Solanki, A. Kumar Singh, S.K. Mishra, S.J. Kennedy, T. Suzuki, Y. Kuroiwa, C. Moriyoshi and D. Pandey, Phys. Rev. B **84**, 144116 (2011).
²⁵ F. Cordero, L. Dalla Bella, F. Corvasce, P.M. Latino and A. Morbidini, Meas. Sci. Technol. **20**, 015702 (2009).
²⁶ A.S. Nowick and B.S. Berry, *Anelastic Relaxation in Crystalline Solids*. (Academic Press, New York, 1972).
²⁷ W. Rehwald, Adv. Phys. **22**, 721 (1973).
²⁸ M.A. Carpenter and E.H.K. Salje, Eur. J. Mineral. **10**, 693 (1998).
²⁹ R. G. Burkovsky, Yu. A. Bronwald, A. V. Filimonov, A. I. Rudskoy, D. Chernyshov, A. Bosak, J. Hlinka, X. Long, Z.-G. Ye, S. B. Vakhrushev, arXiv:1204.5878v1 (2012).
³⁰ H. Yokota, N. Zhang, A.E. Taylor, P.A. Thomas and A.M. Glazer, Phys. Rev. B **80**, 104109 (2009).
³¹ N. Zhang, H. Yokota, A.M. Glazer and P.A. Thomas, Acta Cryst. B **67**, 386 (2011).
³² E.G. Fesenko, V.V. Eremkin and V.G. Smotrakov, Sov. Phys. Solid State **28**, 181 (1986).

- ³³ R.D. Shannon, *Acta Cryst. A* **32**, 751 (1976).
- ³⁴ N.W. Thomas, *Acta Cryst. B* **45**, 337 (1989).
- ³⁵ D. Wang and R.J. Angel, *Acta Cryst. B* **67**, 302 (2011).
- ³⁶ C.J. Howard and H.T. Stokes, *Acta Cryst. B* **54**, 782 (1998).
- ³⁷ H. Zheng, I.M. Reaney, W.E. Lee, N. Jones and H. Thomas, *J. Am. Ceram. Soc.* **85**, 2337 (2002).
- ³⁸ J. Burgy, M. Mayr, V. Martin-Mayor, A. Moreo and E. Dagotto, *Phys. Rev. Lett.* **87**, 277202 (2001).
- ³⁹ E. Dagotto, *New J. Phys.* **7**, 67 (2005).
- ⁴⁰ D.L. Corker, A.M. Glazer, R.W. Whatmore, A. Stallard and F. Fauth, *J. Phys.: Condens. Matter* **10**, 6251 (1998).
- ⁴¹ J. Hlinka, P. Ondrejovic, M. Kempa, E. Borissenko, M. Krisch, X. Long and Z.-G. Ye, *Phys. Rev. B* **83**, 140101 (2011).
- ⁴² D. Viehland, *Phys. Rev. B* **52**, 778 (1995).
- ⁴³ D. Viehland, J.-F. Li, X. Da and Z. Xu, *J. Phys. Chem. Sol.* **57**, 1545 (1996).
- ⁴⁴ J. Ricote, D.L. Corker, R.W. Whatmore, S.A. Impey, A.M. Glazer, J. Dec and K. Roleder, *J. Phys.: Condens. Matter* **10**, 1767 (1998).
- ⁴⁵ Y. Kuroiwa, Y. Terado, S.J. Kim, A. Sawada, Y. Yamamura, S. Aoyagi, E. Nishibori, M. Sakata and M. Takata, *Jpn. J. Appl. Phys.* **44**, 7151 (2005).
- ⁴⁶ B. Ravel and E.A. Stern, *Physica B* **208&209**, 316 (1995).
- ⁴⁷ P. Sollich, V. Heine and M.T. Dove, *J. Phys.: Condens. Matter* **6**, 3171 (1994).
- ⁴⁸ R.W. Whatmore, R. Clarke and A.M. Glazer, *J. Phys. C: Solid State Phys.* **11**, 3089 (1978).
- ⁴⁹ N. Cerereda, B. Noheda, T. Iglesias, J.R. Fernandez - del Castillo, J.A. Gonzalo, N. Duan, Y.L. Wang, D.E. Cox and G. Shirane, *Phys. Rev. B* **55**, 6174 (1997).
- ⁵⁰ X. Dai, Z. Xu, J.-F. Li and D. Viehland, *J. Appl. Phys.* **77**, 3354 (1995).
- ⁵¹ G. Arlt, *Proc. IEEE Ultrasonic Symposium*, 733 (1990).
- ⁵² A.K. Singh, S.K. Mishra, agini, D. Pandey, S. Yoon, S. Baik and N. Shin, *Appl. Phys. Lett.* **92**, 022910 (2008).
- ⁵³ L.A. Reznichenko, L.A. Shilkina, O.N. Razumovskaya, E.A. Yaroslavtseva, S.I. Dudkina, O.A. Demchenko, Yu.I. Yurasov, A.A. Esis and I.N. Andryushina, *Phys. Solid State* **51**, 1010 (2009).
- ⁵⁴ F. Cordero, F. Craciun, F. Trequattrini, E. Mercadelli and C. Galassi, *Phys. Rev. B* **81**, 144124 (2010).
- ⁵⁵ G.O. Jones and P.A. Thomas, *Acta Cryst. B* **58**, 168 (2002).
- ⁵⁶ Y. Hiruma, Y. Watanabe, H. Nagata and T. Takenaka, *Key Eng. Mater.* **350**, 93 (2007).
- ⁵⁷ J. Petzelt, S. Kamba, J. Fbry, D. Noujni, V. Porokhonskyy, A. Pashkin, I. Franke, K. Roleder, J. Suchanicz, R. Klein and G. E. Kugel, *J. Phys.: Condens. Matter* **16**, 2719 (2004).
- ⁵⁸ I.-W. Chen, P. Li and Y. Wang, *J. Phys. Chem. Sol.* **57**, 1525 (1996).
- ⁵⁹ Ph. Ghosez, E. Cockayne, U.V. Waghmare and K.M. Rabe, *Phys. Rev. B* **60**, 836 (1999).
- ⁶⁰ J. Holakovský, *phys. stat. sol. (b)* **56**, 615 (1973).
- ⁶¹ Y. Ishibashi, *J. Phys. Soc. Japan* **63**, 2082 (1994).
- ⁶² M.J. Haun, E. Furman, S.J. Jang and L.E. Cross, *Ferroelectrics* **99**, 13 (1989).
- ⁶³ J. Holakovský, *phys. stat. sol. (b)* **69**, 615 (1975).
- ⁶⁴ I.A. Kornev and L. Bellaiche, *Phys. Rev. B* **79**, 100105 (2009).
- ⁶⁵ N.W. Thomas and A. Beitollahi, *Acta Cryst. B* **50**, 549 (1994).
- ⁶⁶ G.A. Samara, T. Sakudo and K. Yoshimitsu, *Phys. Rev. Lett.* **35**, 1767 (1975).
- ⁶⁷ J. Kreisel, B. Noheda and B. Dkhil, *Phase Trans.* **82**, 633 (2009).
- ⁶⁸ J. Frantti, Y. Fujioka, J. Zhang, S.C. Vogel, Y. Wang, Y. Zhao and R.M. Nieminen, *J. Phys. Chem. B* **113**, 7967 (2009).
- ⁶⁹ G. Fraysse, A. Al-Zein, J. Haines, J. Rouquette, V. Bornand, P. Papet, C. Bogicevic and S. Hull, *Phys. Rev. B* **84**, 144110 (2011).
- ⁷⁰ N. L. Ross, Zhao and R. J. Angel, *J. Solid State Chem.* **177**, 1276 (2004).
- ⁷¹ J. Zhao, N.L. Ross and R.J. Angel, *Acta Cryst. B* **60**, 263 (2004).
- ⁷² B. Magyar-Köpe, L. Vitos, B. Johansson and J. Kollár, *Phys. Rev. B* **66**, 092103 (2002).
- ⁷³ R.J. Angel, J. Zhao and N.L. Ross, *Phys. Rev. Lett.* **95**, 025503 (2005).
- ⁷⁴ W. Zhong and D. Vanderbilt, *Phys. Rev. Lett.* **74**, 2587 (1995).
- ⁷⁵ P. Yang, M.A. Rodriguez, G.R. Burns, M.E. Stavig and R.H. Moore, *J. Appl. Phys.* **95**, 3626 (2004).
- ⁷⁶ D. Wang, J. Weerasinghe, L. Bellaiche and J. Hlinka, *Phys. Rev. B* **83**, 020301 (2011).
- ⁷⁷ J. Weerasinghe, D. Wang and L. Bellaiche, *Phys. Rev. B* **85**, 014301 (2012).